

NMR study of magnetic and nonmagnetic impurities in $\text{YBa}_2\text{Cu}_4\text{O}_8$

G. V. M. Williams and J. L. Tallon

The New Zealand Institute for Industrial Research, P.O. Box 31310, Lower Hutt, New Zealand

R. Dupree

Department of Physics, University of Warwick, Coventry CV4 7AL, United Kingdom

(Received 5 November 1998; revised manuscript received 18 August 1999)

We report ^{89}Y and ^{17}O NMR measurements on $\text{YBa}_2\text{Cu}_4\text{O}_8$ doped with Ni and Zn impurities to investigate the effect of magnetic and nonmagnetic impurities on superconductivity and on the normal state. We find that Zn induces extra NMR peaks in both the ^{89}Y and ^{17}O NMR spectra attributed to nuclei near the Zn impurity while the Ni moment washes out the NMR signal from nuclei near the Ni impurity. The ^{89}Y NMR shift from ^{89}Y sites nearest neighbor and next-nearest neighbor to the Zn impurity can be modeled in terms of a Curie-like NMR shift from Cu sites adjacent to the Zn impurity. However, the temperature dependence of the NMR linewidths and modeling of the NMR spectra are inconsistent with a commensurate spin-density oscillation about a local moment induced by Zn or about the Ni moment. We find that the normal-state pseudogap is very locally suppressed over a range of just one lattice parameter.

INTRODUCTION

While high temperature superconductivity research has been ongoing for over thirteen years, there is still controversy surrounding the effect of magnetic Ni and nonmagnetic Zn impurities in the cuprates.¹⁻⁷ The underlying antiferromagnetic correlations in the superconducting CuO_2 planes makes the understanding of the effect of magnetic and nonmagnetic impurities crucial for the development of theories to describe superconductivity in the high temperature superconducting cuprates. For example, it was observed that T_c is decreased much more rapidly by Zn than Ni in $\text{YBa}_2\text{Cu}_3\text{O}_{7-\delta}$ which resulted in Zn being described as a superunitary scatterer and Ni being described as a Born scatterer.¹ However susceptibility measurements on Zn and Ni substituted $\text{YBa}_2\text{Cu}_4\text{O}_8$ and $\text{La}_{1-x}\text{Sr}_x\text{CuO}_4$ show that Ni and Zn depress T_c by the same amount.^{8,9} Furthermore, muon spin rotation measurements (μSR) on $\text{Y}_{1-x}\text{Ca}_x(\text{Cu}_{1-z}\text{Zn}_z)_3\text{O}_{7-\delta}$ and $\text{La}_{2-x}\text{Sr}_x\text{Cu}_{1-z}\text{Zn}_z\text{O}_4$ have clearly shown that Zn is a unitary scatterer⁴ in both the under and overdoped regions. This discrepancy may be trivially due to Ni only partially substituting for Cu in the CuO_2 planes of the $\text{YBa}_2\text{Cu}_3\text{O}_{7-\delta}$ superconductor.^{10,11}

The effect of these substituents on the normal-state properties is equally confusing. Previous ^{89}Y nuclear magnetic resonance (NMR) measurements on $\text{YBa}_2(\text{Cu}_{1-z}\text{Zn}_z)\text{O}_{7-\delta}$ have been consistently analyzed in terms of a Curie-like contribution from the Cu sites nearest neighbor to the Zn impurity.² This Curie-like contribution was attributed to an induced local moment observed in μSR (Ref. 6) and susceptibility measurements² on $\text{YBa}_2(\text{Cu}_{1-z}\text{Zn}_z)_3\text{O}_{7-\delta}$ and existing up to, and above, room temperature. However, recent μSR measurements on a series of $\text{YBa}_2(\text{Cu}_{1-z}\text{Zn}_z)_4\text{O}_8$ samples with different Zn contents found no evidence for an additional local moment induced by Zn which is discernible above the background.⁷ Susceptibility measurements on good-quality $\text{YBa}_2(\text{Cu}_{1-z}\text{Zn}_z)_3\text{O}_{7-\delta}$ samples indicate that there is no local moment induced by Zn for temperatures

≥ 150 K.^{12,13} However, the susceptibility data indicate the development of a Curie-like term associated with Zn for temperatures less than 150 K. Measurements of the ^{17}O NMR linewidth on $\text{YBa}_2(\text{Cu}_{1-z}\text{Ni}_z)\text{O}_{7-\delta}$ (Ref. 14) and ^{63}Cu NMR linewidth on $\text{YBa}_2(\text{Cu}_{1-z}\text{Zn})\text{O}_{7-\delta}$ (Ref. 15) samples have been analyzed in terms of a commensurate spin density oscillation induced by the Ni or Zn impurities where the extent of this oscillation is determined by the antiferromagnetic correlation length. However, attributing the temperature-dependent NMR linewidths to a spin density oscillation has recently been questioned.⁹

In this paper we report ^{89}Y and ^{17}O NMR measurements on $\text{YBa}_2(\text{Cu}_{1-z}\text{Zn}_z)_4\text{O}_8$, $\text{YBa}_2(\text{Cu}_{1-z}\text{Ni}_z)_4\text{O}_8$ and $\text{YBa}_2(\text{Cu}_{1-z}\text{Ni}_y\text{Zn}_{z-y})_4\text{O}_8$ superconductors and address the above issues.

The underdoped $\text{YBa}_2\text{Cu}_4\text{O}_8$ compound is an ideal high temperature superconductor for investigating the effect of impurities because, unlike $\text{YBa}_2\text{Cu}_3\text{O}_{7-\delta}$, it is stoichiometric with a fixed oxygen content. In underdoped $\text{YBa}_2\text{Cu}_3\text{O}_{7-\delta}$ with a hole concentration similar to that of $\text{YBa}_2\text{Cu}_4\text{O}_8$, the effect of oxygen disorder is to asymmetrically broaden the NMR resonance. We show below that the $\text{YBa}_2(\text{Cu}_{1-z}\text{Zn}_z)_4\text{O}_8$ ^{89}Y NMR spectra contain three peaks similar to those observed in $\text{YBa}_2(\text{Cu}_{1-z}\text{Zn}_z)\text{O}_{6.64}$ and that ^{17}O NMR spectra are consistent with a Curie-like contribution from Cu sites nearest neighbor to the Zn impurity. However ^{89}Y and ^{17}O NMR measurements on $\text{YBa}_2(\text{Cu}_{1-z}\text{Ni}_z)_4\text{O}_8$ indicate a significant broadening from ^{89}Y and ^{17}O near the Ni impurity and a broadening comparable to that of Zn for sites away from the Ni impurity. The cosubstitution of Zn and Ni clearly shows that the dramatic decrease in T_c is not related to magnetic moments or a local suppression of the antiferromagnetic spin correlations. Furthermore, the results are inconsistent with a commensurate spin density oscillation about either the Zn or Ni substituent with an extent determined by the antiferromagnetic correlation length. Our results indicate an urgent need to reassess

theoretical scenarios based on Zn and Ni substitution in the superconducting cuprates.

EXPERIMENTAL DETAILS

$\text{YBa}_2(\text{Cu}_{1-z}\text{Zn}_z)_4\text{O}_8$, $\text{YBa}_2(\text{Cu}_{1-z}\text{Ni}_z)_4\text{O}_8$ and $\text{YBa}_2(\text{Cu}_{1-z}\text{Zn}_{z/2}\text{Ni}_{z/2})_4\text{O}_8$ ceramic samples were synthesized from a stoichiometric mix of Y_2O_3 , $\text{Ba}(\text{NO}_3)_2$, CuO , NiO , and ZnO after decomposing in air at 700°C for 1 h. The samples were sintered in 60 bars O_2 at 930°C for 6 h, 940°C for 24 h, and 940°C for 48 h. The $\text{YBa}_2(\text{Cu}_{1-z}\text{Ni}_z)_4\text{O}_8$ and $\text{YBa}_2(\text{Cu}_{1-z}\text{Zn}_{z/2}\text{Ni}_{z/2})_4\text{O}_8$ samples were sintered for a further four times at 940°C for 48 h to ensure complete impurity homogeneity. X-ray diffraction (XRD) measurements showed no evidence of impurity phases. AC susceptibility was used to measure the T_c values.

Samples for ^{17}O NMR were ^{17}O exchanged in 10% ^{17}O enriched O_2 at 700°C for 6 h. The samples were then magnetically aligned at 1 T in a resin and the alignments were confirmed by XRD. The alignment was required because ^{17}O has a $I=5/2$ nuclear spin and hence a quadrupole moment. In the $\text{YBa}_2\text{Cu}_4\text{O}_8$ powder the Zeeman and quadrupole interactions result in a broad NMR powder pattern while measurements on crystals with the magnetic field parallel to the c -axis result in well-defined peaks and four well-separated satellite peaks.

^{17}O NMR measurements were performed at temperatures from 100 to 300 K using a continuous-flow cryostat in a magnetic field of 8.45 T where the c axis was parallel to the applied magnetic field. The spectra were obtained using the 90° - τ - 180° pulse sequence where the 90° pulse width was 2 μs . The time delay between each pulse sequence, D_0 , was varied from 50 ms to 5 s to investigate different spectral components with different spin lattice relaxation rates, $1/^{17}T_1$. Small values of D_0 saturate spectral components with $^{17}T_1 > D_0$. The spectra were referenced to H_2O .

^{89}Y NMR magic angle spinning (MAS) measurements were made between 130 and 350 K and a rotor frequency of >2.5 kHz using a Varian Unity 500 spectrometer and an 11.74 T superconducting magnet. The advantage of MAS is that it can significantly reduce the NMR linewidth by reducing the spin-spin broadening. The 90° - τ - 180° pulse sequence was used with τ being set to one rotor period. The NMR shifts were referenced to a 1 M aqueous solution of YCl_3 .

RESULTS AND ANALYSIS

We show in Fig. 1 that T_c is rapidly and equally depressed by Ni, Zn, or Ni:Zn substitution in $\text{YBa}_2\text{Cu}_4\text{O}_8$. Here we plot T_c against Zn content for $\text{YBa}_2(\text{Cu}_{1-z}\text{Zn}_z)_4\text{O}_8$ (open down triangles),⁹ $\text{YBa}_2(\text{Cu}_{1-z}\text{Ni}_z)_4\text{O}_8$ (open up triangles),⁹ and $\text{YBa}_2(\text{Cu}_{1-z}\text{Zn}_{z/2}\text{Ni}_{z/2})_4\text{O}_8$ (filled circles). This similar behavior indicates that the pair-breaking mechanism does not depend on a Ni magnetic moment or a possible local suppression of the antiferromagnetic correlations about the Zn impurity as previously suggested. We also show in Fig. 1 that the equal depression of T_c by Ni and Zn impurities is not limited to the $\text{YBa}_2\text{Cu}_4\text{O}_8$ compound but is evident also in $\text{La}_{1-x}\text{Sr}_x\text{CuO}_4$. This important result is little recognized in the field and needs to be strongly emphasized. It is consistent with the interpretation of μSR data where Zn and Ni were

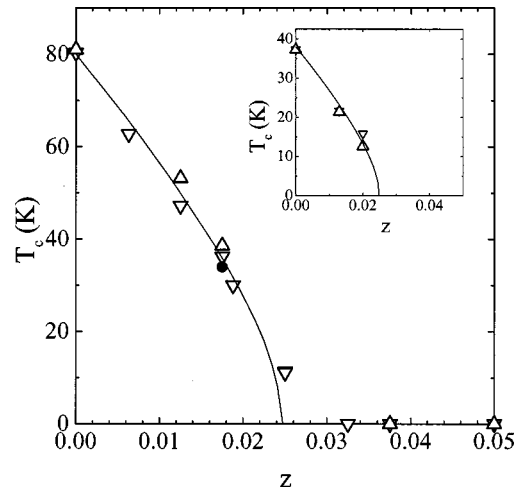


FIG. 1. Plot of the T_c against impurity concentration z for $\text{YBa}_2(\text{Cu}_{1-z}\text{Zn}_z)_4\text{O}_8$ (open down triangle) (Ref. 9), $\text{YBa}_2(\text{Cu}_{1-z}\text{Ni}_z)_4\text{O}_8$ (open up triangle) (Ref. 9), and $\text{YBa}_2(\text{Cu}_{1-z}\text{Zn}_{z/2}\text{Ni}_{z/2})_4\text{O}_8$ (filled circle). Inset: Plot of T_c against impurity concentration z for $\text{La}_{1.85}\text{Sr}_{0.15}\text{Cu}_{1-z}\text{Zn}_z\text{O}_4$ (open up triangle) and $\text{La}_{1.85}\text{Sr}_{0.15}\text{Cu}_{1-z}\text{Ni}_z\text{O}_4$ (open up triangle). The solid curves are obtained from the Abrikosov-Gorkov equation.

both described as unitary pairbreakers in a superconductor with a $d_{x^2-y^2}$ order parameter.⁴ We show in Fig. 1 that the T_c suppression can be fitted to the Abrikosov-Gorkov equation (solid curve) in a manner similar to that for $\text{Y}_{1-x}\text{Ca}_x\text{Ba}_2(\text{Cu}_{1-z}\text{Zn}_z)_3\text{O}_{7-\delta}$ samples.⁴ The more rapid reduction in T_c in the case of $\text{YBa}_2\text{Cu}_4\text{O}_8$ reflects the underdoped state of this compound.^{16,17}

We first consider the ^{89}Y and ^{17}O NMR spectra from $\text{YBa}_2(\text{Cu}_{0.9825}\text{Zn}_{0.0175})_4\text{O}_8$ and show below that the data can be interpreted in terms of a Curie-like spin susceptibility arising from only those Cu sites nearest neighbor to the Zn impurity. It can be seen in Fig. 2 that the ^{89}Y NMR spectra display three peaks with a temperature-dependent shift. Here we present ^{89}Y NMR spectra from $\text{YBa}_2(\text{Cu}_{0.9825}\text{Zn}_{0.0175})_4\text{O}_8$ at (a) 132 K, (b) 192 K, (c) 220 K, and (d) 293 K. The appearance of three peaks is consistent with ^{89}Y NMR measurements on $\text{YBa}_2(\text{Cu}_{1-z}\text{Zn}_z)\text{O}_{6.64}$ by Mahajan *et al.*;² however, the peaks are sharper in the impurity substituted $\text{YBa}_2\text{Cu}_4\text{O}_8$ samples because of the MAS technique and the highly ordered state of this compound. The three peaks in the ^{89}Y NMR spectra from $\text{YBa}_2(\text{Cu}_{0.9825}\text{Zn}_{0.0175})_4\text{O}_8$ shown in Fig. 2 also have different $^{89}T_1$ values as previously found by Mahajan *et al.* from ^{89}Y NMR measurements on $\text{YBa}_2(\text{Cu}_{1-z}\text{Zn}_z)\text{O}_{6.64}$. This is apparent in Fig. 3 where we plot ^{89}Y NMR spectra from $\text{YBa}_2(\text{Cu}_{0.9825}\text{Zn}_{0.0175})_4\text{O}_8$ at 133 K with (a) $D_0=10$ s and (b) $D_0=60$ s. There is a significant change in the intensities of the satellite peaks relative to the central peak. We show in Figs. 2 and 3 that the ^{89}Y NMR spectra can be fitted to three Gaussians line shapes (dashed curves). The resultant peak positions are plotted in Fig. 4 for the main peak (open circles), first satellite (open down triangles), and second satellite (open up triangles). It can be seen from the inset to Fig. 4 that the linewidths consistently increase when going from the main peak to the second satellite peak.

The ^{89}Y NMR shifts from all three peaks shown in Fig. 4 clearly have different temperature dependencies. We show in

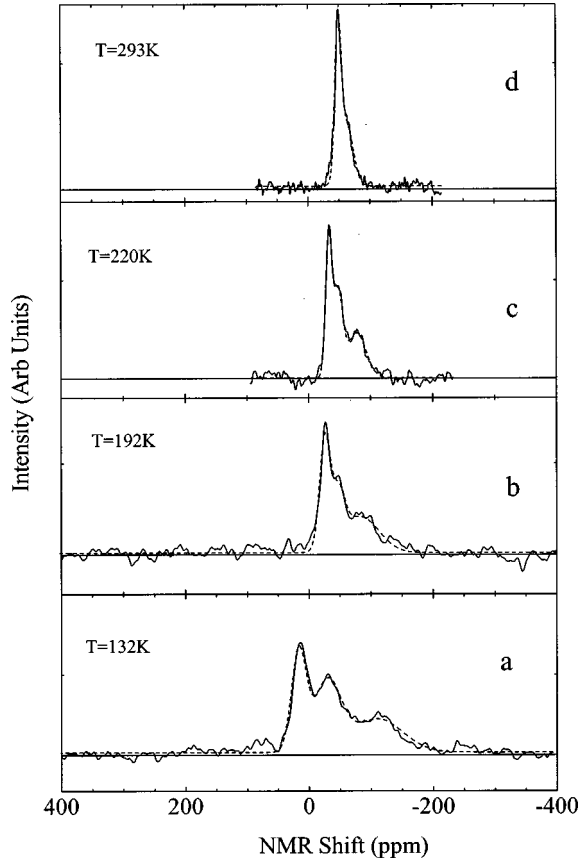


FIG. 2. Plot of the $\text{YBa}_2(\text{Cu}_{0.9825}\text{Zn}_{0.0175})_4\text{O}_8$ ^{89}Y NMR MAS spectra at (a) 132 K, (b) 192 K, (c) 220 K, and (d) 293 K. The dashed curves are fits to the data as described in the text.

Fig. 4 that the ^{89}Y NMR shifts can be modeled in a manner similar to that for $\text{YBa}_2(\text{Cu}_{1-z}\text{Zn}_z)\text{O}_{6.64}$ by Mahajan *et al.* with satellite 2 originating from ^{89}Y nearest neighbor to the Zn impurity, satellite 1 originating from ^{89}Y next-nearest neighbor to the Zn impurity, and the main line originating from all other ^{89}Y sites. To show this, we first note that the NMR shift as deduced from the Mila-Rich Hamiltonian¹⁸ can be expressed as¹⁹

$$K = \frac{\sum_j A_j}{g\mu_B} \chi_s + \sigma, \quad (1)$$

where A_j are the hyperfine coupling constants (negative for ^{89}Y), g is the Landé factor, μ_B is the Bohr magneton, χ_s is the static spin susceptibility per CuO_2 plane unit, and σ is the temperature-independent chemical shift. It has previously been shown that $^{89}\text{K}_s$, $^{17}\text{K}_s$, and $^{63}\text{K}_s$ all have the same temperature dependence and within the Mila-Rice model the ^{89}Y NMR interaction is via transferred hyperfine coupling to the spins on the eight nearest-neighbor Cu while the ^{17}O NMR interaction is via transferred hyperfine coupling to the spins on the two nearest-neighbor Cu atoms. The temperature dependence of the NMR shift in underdoped cuprates is typified by the ^{89}Y NMR spectra from $\text{YBa}_2\text{Cu}_4\text{O}_8$ plotted in Fig. 4 (solid curve) where the decrease in the spin susceptibility has been attributed to a normal-state pseudogap that disappears at higher hole concentrations, p , greater than ~ 0.19 .

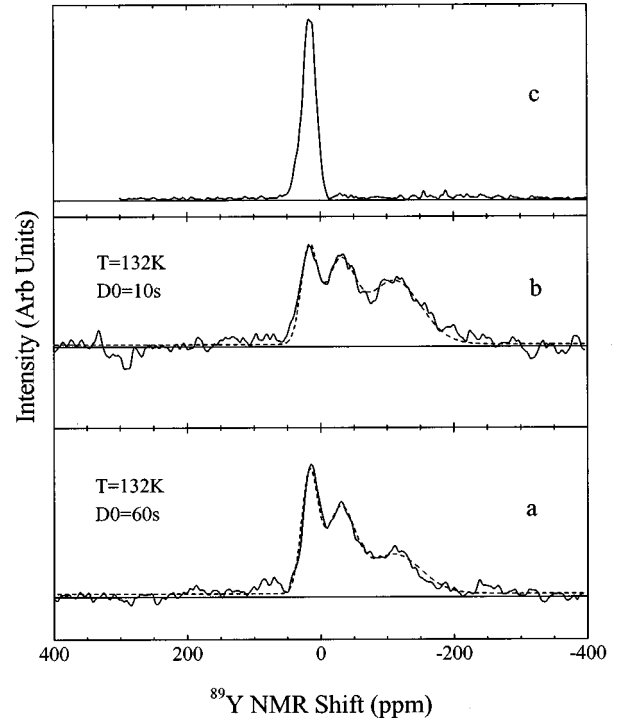


FIG. 3. Plot of the $\text{YBa}_2(\text{Cu}_{0.9825}\text{Zn}_{0.0175})_4\text{O}_8$ ^{89}Y NMR MAS spectra at 132 K and D_0 of (a) 60 s and (b) 10 s. The dashed curves are fits to the data as described in the text. Also shown (c) is the expected spectrum if Zn induced a local moment on the Cu atom nearest neighbor to the Zn impurity and the induced local moment also caused a spin density oscillation as described in the text.

In the model of Mahajan *et al.* the NMR shift for the main line, ^{89}K , the first satellite, $^{89}\text{K}_1$, and the second satellite, $^{89}\text{K}_2$, can be written as

$$^{89}\text{K} = ^{89}\text{K}_s + ^{89}\sigma, \quad (2a)$$

$$^{89}\text{K}_1 = \frac{7}{8} ^{89}\text{K}_s + \frac{^{89}\text{C}}{T} + ^{89}\sigma, \quad (2b)$$

$$^{89}\text{K}_2 = \frac{5}{8} ^{89}\text{K}_s + \frac{2}{T} ^{89}\text{C} + ^{89}\sigma, \quad (2c)$$

where $^{89}\text{K}_s$ is the bulk Knight shift, ^{89}C is the constant describing a Curie-like temperature dependence, T is the temperature, and $^{89}\sigma$ is the temperature-independent chemical shift. We show in Fig. 4 by the dashed curves that Eq. (2) does describe the data. It should be noted that the inclusion of only a Curie-like temperature dependence from the nearest neighbor Cu sites implies a very local suppression of the normal state pseudogap. We used $^{89}\text{K}_s$ from $\text{YBa}_2\text{Cu}_4\text{O}_8$ for the bulk Knight shift and a bulk chemical shift of $^{89}\sigma = -165$ ppm. We note that $^{89}\sigma = -165$ ppm is within the range of experimental values^{20,21} and is the value deduced from a recent study of ^{89}Y and ^{63}Cu NMR data.²² The best fit is obtained with $^{89}\text{C} = (11900 \pm 1000)$ ppm K and $^{89}\sigma = -153$ ppm from the nearest-neighbor site and $^{89}\sigma = -176$ ppm from the next-nearest-neighbor site. The Curie-like prefactor is comparable to that obtained from underdoped $\text{YBa}_2(\text{Cu}_{1-z}\text{Zn}_z)\text{O}_{6.64}$ single crystals (13100 ppm K for $H\parallel c$ and 11600 ppm K for $H\parallel ab$).

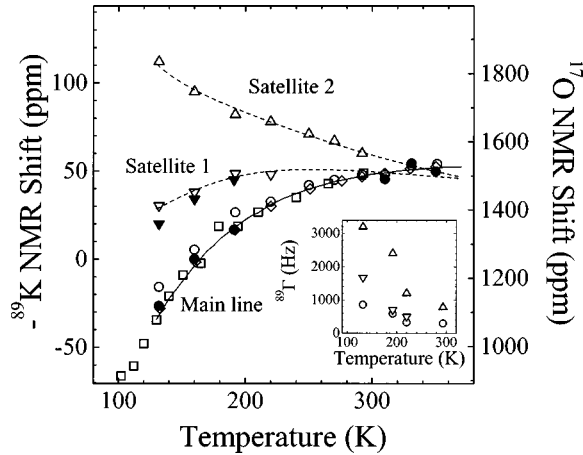


FIG. 4. Plot of the ^{89}Y NMR shift against temperature for the $\text{YBa}_2(\text{Cu}_{0.9825}\text{Zn}_{0.0175})_4\text{O}_8$ main peak (open circle), $\text{YBa}_2(\text{Cu}_{0.9825}\text{Zn}_{0.0175})_4\text{O}_8$ first satellite (open down triangle), $\text{YBa}_2(\text{Cu}_{0.9825}\text{Zn}_{0.0175})_4\text{O}_8$ second satellite (open up triangle), $\text{YBa}_2(\text{Cu}_{0.9825}\text{Ni}_{0.0175})_4\text{O}_8$ main peak (open diamond), the $\text{YBa}_2(\text{Cu}_{0.9825}\text{Zn}_{0.00875}\text{Ni}_{0.00875})_4\text{O}_8$ main peak (filled circle), and $\text{YBa}_2(\text{Cu}_{0.9825}\text{Zn}_{0.00875}\text{Ni}_{0.00875})_4\text{O}_8$ first satellite (filled down triangle). Also included is the ^{89}Y NMR shift from $\text{YBa}_2\text{Cu}_4\text{O}_8$ (solid curve) and the ^{17}O NMR shift from $\text{YBa}_2(\text{Cu}_{0.9825}\text{Zn}_{0.00875}\text{Ni}_{0.00875})_4\text{O}_8$ (open square) with $H\parallel c$. The dashed curves are fits to the data using the model described in the text. Inset: plot of the ^{89}Y NMR linewidths, $^{89}\Gamma$, plotted against temperature for the $\text{YBa}_2(\text{Cu}_{0.9825}\text{Zn}_{0.0175})_4\text{O}_8$ main peak (open circle), first satellite (open down triangle) and second satellite (open up triangle), as obtained by fitting the NMR data in Fig. 2.

Mahajan *et al.* attributed the satellite peaks in the $\text{YBa}_2(\text{Cu}_{1-z}\text{Zn}_z)\text{O}_{6.64}$ ^{89}Y NMR spectra to an induced local moment on the four nearest-neighbor Cu sites to the Zn impurity. In this interpretation, a local moment can be deduced from ^{89}C by noting that for a local moment, χ_s in Eq. (1) reduces to $\chi_s = p^2/(3k_B T)$ where k_B is the Boltzmann constant and p is the magnitude of the local moment. Inserting this χ_s into Eq. (1) gives $p = (3gk_B^{89}\text{C}/|^{89}\text{A}|)^{1/2}$ where ^{89}A is the hyperfine coupling constant. To obtain an estimate of p within the Mahajan *et al.* interpretation we use the bulk ^{89}A value of $^{89}\text{A} = -0.39\text{ T}$ (Ref. 19) and from $^{89}\text{C} = 11900\text{ ppm K}$ we obtain $p = 0.52\mu_B$ and hence a local moment per Zn atom of $1.04\mu_B/\text{Zn}$. The deduced local moment is comparable to that found by Mahajan *et al.* from susceptibility measurements on $\text{YBa}_2(\text{Cu}_{1-z}\text{Zn}_z)\text{O}_{6.64}$ ($0.86\mu_B/\text{Zn}$). This, and the excellent fit to the ^{89}Y NMR shift of the peaks in the $\text{YBa}_2(\text{Cu}_{1-z}\text{Zn}_z)_4\text{O}_8$ ^{89}Y NMR spectra, would appear to provide support for the Zn-induced local moment model. However, as mentioned earlier, recent μSR measurements on $\text{YBa}_2(\text{Cu}_{1-z}\text{Zn}_z)_4\text{O}_8$ found no evidence of a local moment induced by Zn over and above the intrinsic moment present in the pure compound. Furthermore, susceptibility measurements deduce widely different values for the induced local moment ranging from 0 to $\sim 1\mu_B/\text{Zn}$.^{2,13,15,23} These conflicting results indicate that further experimental and theoretical research on this issue is required. We speculate that a final picture will probably incorporate two ideas: (i) the Curie-like term does not derive from a local moment; and (ii) the Zn-induced term is associated with the normal-state pseudogap,¹² disappearing at

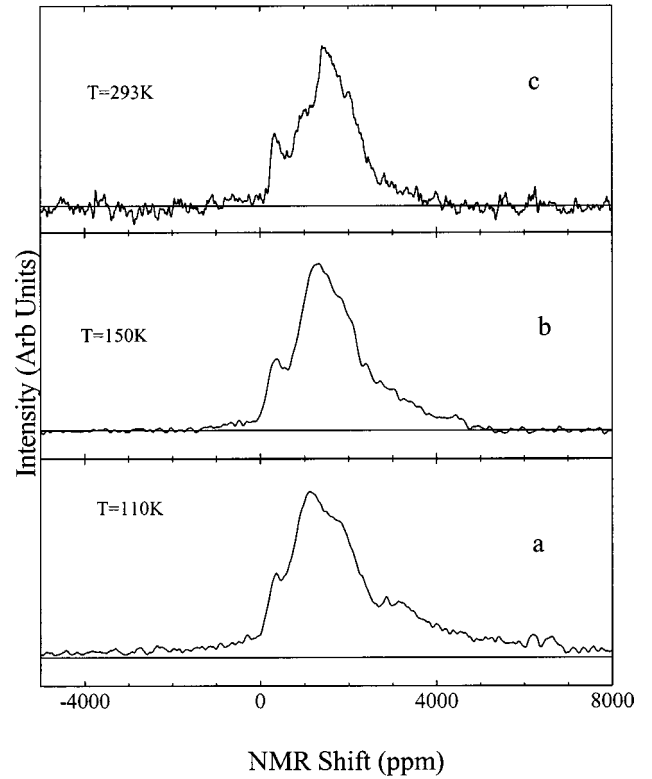


FIG. 5. Plot of the $\text{YBa}_2(\text{Cu}_{0.9825}\text{Zn}_{0.0175})_4\text{O}_8$ ($-1/2, 1/2$) ^{17}O NMR spectra at (a) 110 K, (b) 150 K, and (c) 293 K for $H\parallel c$.

temperatures $T > E_g/k_B$ or for hole concentrations $p > 0.19$ where the normal state pseudogap is zero.¹⁶

Previous NMR studies on $\text{YBa}_2(\text{Cu}_{1-z}\text{Zn}_z)_3\text{O}_{7-\delta}$ have also invoked an induced local moment with a commensurate spin density oscillation to account for the increasing NMR linewidth with decreasing temperature.^{2,15} We have attempted to model our $\text{YBa}_2(\text{Cu}_{1-z}\text{Zn}_z)_4\text{O}_8$ ^{89}Y NMR data near 130 K in a manner similar to the analysis of ^{63}Cu NMR data by Walstedt *et al.*¹⁵ using a commensurate spin density oscillation of the form $S(i, j) \propto (-1)^{i+j} \exp(-(i^2 + j^2)/(4\xi^2))$ where ξ is the antiferromagnetic correlation length in units of the average ab unit cell length, a . We used $\xi = 4a$ (close to that deduced at 130 K by modeling of the NMR data²⁴) and simulated the upper and lower CuO_2 planes using two 100 by 100 grids. We find that the resultant spectra only contain a single main peak where the satellite peaks have been washed out into a very broad background. This is apparent in Fig. 3(c) where we show the simulated ^{89}Y NMR data at 132 K. While the linewidth of the main peak is close to that in the sample it can be seen that the satellite peaks are completely washed out.

Unlike the previous study on $\text{YBa}_2(\text{Cu}_{1-z}\text{Zn}_z)_3\text{O}_{7-\delta}$ we have also performed ^{17}O NMR measurements and present in Fig. 5 ^{17}O NMR data on aligned $\text{YBa}_2(\text{Cu}_{0.9825}\text{Zn}_{0.0175})_4\text{O}_8$ with the c axis parallel to the magnetic field and at (a) 110 K, (b) 150 K, and (c) 293 K. As the low-temperature spectrum is very broad, resonance data were taken at 50 kHz (~ 1000 ppm) intervals and the resultant magnitude spectra were summed. We first consider the room temperature spectra in Fig. 5(c). By comparison with previous NMR studies on $\text{YBa}_2\text{Cu}_3\text{O}_{7-\delta}$,^{25,26} we attribute the main peak in the ^{17}O NMR spectra to the central ($-1/2, +1/2$) transitions from

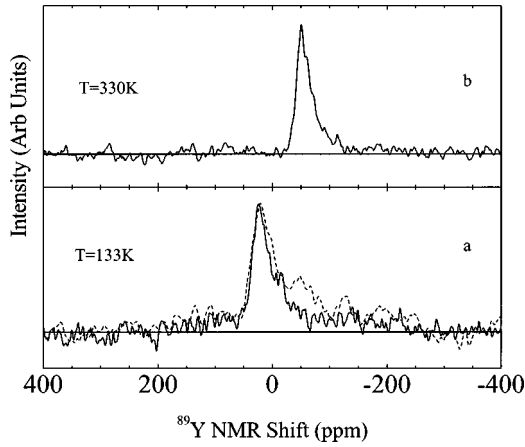


FIG. 6. Plot of the ^{89}Y NMR MAS spectra from (a) $\text{YBa}_2(\text{Cu}_{0.9825}\text{Ni}_{0.0175})_4\text{O}_8$ at 133 K and $D_0=60$ s (dashed curve) and $\text{YBa}_2(\text{Cu}_{0.9825}\text{Ni}_{0.0175})_4\text{O}_8$ at 133 K and $D_0=10$ s (solid curve) and (b) $\text{YBa}_2(\text{Cu}_{0.9825}\text{Ni}_{0.0175})_4\text{O}_8$ at 330 K and $D_0=20$ s.

the O2, O3 sites in the CuO_2 planes (~ 1500 ppm). The other peaks can be attributed to the central and satellite transitions from the O1 chain site and the O4 apical site. This site assignment was confirmed by increasing D_0 from 50 ms to 2 s where the O4 and O1 intensities increased indicating a larger spin-lattice relaxation time, $^{17}T_1$, as previously observed. The relative intensities of each peak depend on the site disorder and the degree of ^{17}O exchange on each site. It is clear in Fig. 5(a) that the spectra are broader and another broad peak appears at lower temperatures (~ 3000 ppm at 110 K). We show below that this peak can be attributed to ^{17}O near the Zn impurity. We note that the O1 peak near 1760 ppm precludes us from accurately determining the temperature dependence of the O2, O3 peak.

By comparison with the modeling of the ^{89}Y NMR data we would expect the positions of the ^{17}O main and satellite peaks, ^{17}K , $^{17}K_1$ and $^{17}K_2$ to be at

$$^{17}K = ^{17}K_s + ^{17}\sigma, \quad (3a)$$

$$^{17}K_1 = \frac{1}{2} ^{17}K_s + \frac{^{17}C}{T} + ^{17}\sigma, \quad (3b)$$

$$^{17}K_2 = \frac{^{17}C}{T} + ^{17}\sigma, \quad (3c)$$

where $^{17}K_s$ is the bulk Knight shift, ^{17}C is the constant describing a Curie-like temperature dependence, and $^{17}\sigma$ is the temperature-independent chemical shift. However, because the satellite peak is broad (~ 2400 ppm at 110 K) and $^{17}K_s/2$ is small (~ 470 ppm) we expect that the first and second satellites would merge into one peak with a NMR shift of

$$^{17}K \approx \frac{1}{4} ^{17}K_s + \frac{^{17}C}{T} + ^{17}\sigma. \quad (4)$$

From the position of the satellite peak at 110 K and using $^{17}\sigma=250$ ppm (Ref. 27) we deduce that $^{17}C=(2.8 \pm 0.3) \times 10^5$ (ppm K). From the known hyperfine coupling constants this corresponds to $^{89}C=(10700 \pm 1100)$ (ppm K) which is comparable to that deduced from the ^{89}Y NMR data.

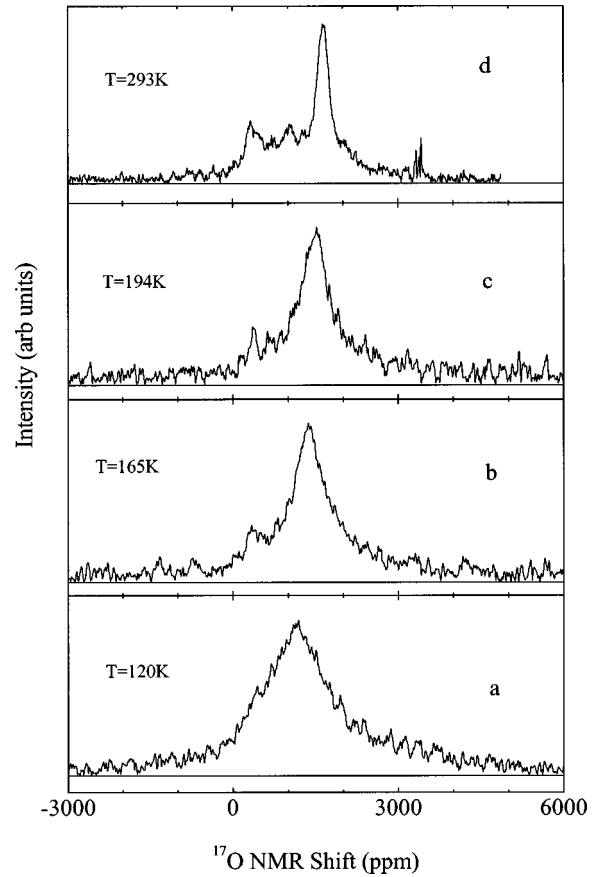


FIG. 7. Plot of the $\text{YBa}_2(\text{Cu}_{0.9825}\text{Ni}_{0.0175})_4\text{O}_8$ ($-1/2, 1/2$) ^{17}O NMR spectra at (a) 120 K, (b) 165 K (c) 194 K, and (d) 293 K for $H \parallel c$.

The effect of Ni on the ^{89}Y and ^{17}O NMR spectra for $\text{YBa}_2(\text{Cu}_{1-z}\text{Ni}_z)_4\text{O}_8$ is in stark contrast to that found when Zn is substituted into $\text{YBa}_2\text{Cu}_4\text{O}_8$. This is apparent in Fig. 6 where we plot the $\text{YBa}_2(\text{Cu}_{0.9825}\text{Ni}_{0.0175})_4\text{O}_8$ ^{89}Y NMR spectra at (a) 133 K with $D_0=60$ s (solid curve), 133 K with $D_0=10$ s (dashed curve) and (b) at 330 K with $D_0=20$ s. There is a strong asymmetric broadening that is absent in the pure compound and the spectra are broader at low temperatures. There is also a very broad resonance at low temperatures. It can be seen by the dashed curve in Fig. 6(a) that there is also a fast relaxing component in the region where $\text{YBa}_2(\text{Cu}_{0.9825}\text{Zn}_{0.0175})_4\text{O}_8$ satellite peaks are observed, however, the fast relaxing component is broader and the relative intensity is significantly less than that observed in $\text{YBa}_2(\text{Cu}_{0.9825}\text{Zn}_{0.0175})_4\text{O}_8$. By comparison with the $\text{YBa}_2(\text{Cu}_{0.9825}\text{Zn}_{0.0175})_4\text{O}_8$ ^{89}Y NMR spectra, we attribute the fast relaxing component to ^{89}Y near the Ni impurity which is being significantly broadened by the Ni moment [$1.5\mu_B/\text{Ni}$ to $3.4\mu_B/\text{Ni}$ (Refs. 28–30)]. This interpretation is strengthened in Fig. 4 by noting that the ^{89}Y NMR shift of the $\text{YBa}_2(\text{Cu}_{0.9825}\text{Ni}_{0.0175})_4\text{O}_8$ central line (filled circles) is close to that found in both the pure compound and from the ^{89}Y NMR peak in $\text{YBa}_2(\text{Cu}_{0.9825}\text{Zn}_{0.0175})_4\text{O}_8$ attributed to ^{89}Y from the bulk. We find that the ^{89}Y NMR data cannot be interpreted in terms of the commensurate spin density oscillation used to model ^{17}O NMR linewidth data from $\text{YBa}_2(\text{Cu}_{1-z}\text{Ni}_z)_3\text{O}_{7-\delta}$. The value of $\xi \sim 4a$ expected at this temperature for $\text{YBa}_2(\text{Cu}_{0.9825}\text{Ni}_{0.0175})_4\text{O}_8$ will produce spec-

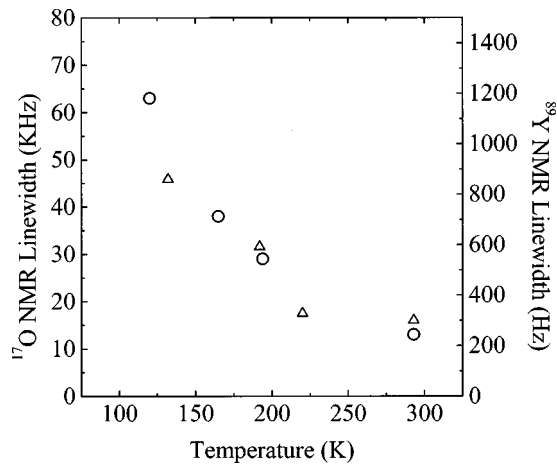


FIG. 8. Plot of the O2O3 ^{17}O NMR linewidths against temperature for $\text{YBa}_2(\text{Cu}_{0.9825}\text{Ni}_{0.0175})_4\text{O}_8$ (open circle). Also included is the ^{89}Y NMR main peak linewidth for $\text{YBa}_2(\text{Cu}_{0.9825}\text{Zn}_{0.0175})_4\text{O}_8$ (open triangle).

tra similar to that of Fig. 3(c) where, just as for Zn in $\text{YBa}_2(\text{Cu}_{0.9825}\text{Zn}_{0.0175})_4\text{O}_8$, the signal near the Ni moment is washed out by the spin density oscillation resulting in no visible satellite peaks. However, the existence of a component in the region of the $\text{YBa}_2(\text{Cu}_{0.9825}\text{Zn}_{0.0175})_4\text{O}_8$ satellite peaks indicates that any commensurate spin density oscillation will be very localized with ξ much less than $4a$.

It is clear from the $\text{YBa}_2(\text{Cu}_{0.9825}\text{Ni}_{0.0175})_4\text{O}_8$ ^{17}O NMR data plotted in Fig. 7 that there is a strong temperature-dependent broadening of the central peak. Here we plot ^{17}O NMR data with $c\parallel H$ from $\text{YBa}_2(\text{Cu}_{0.9825}\text{Ni}_{0.0175})_4\text{O}_8$ at (a) 120 K, (b) 165 K, (c) 195 K, and (d) 293 K. From these spectra the temperature dependence of the ^{17}O NMR shift for O2, O3 is plotted in Fig. 4 (open squares) and is seen to be comparable to that from the central line in the $\text{YBa}_2(\text{Cu}_{0.9825}\text{Ni}_{0.0175})_4\text{O}_8$ ^{89}Y NMR spectra. The corresponding ^{17}O NMR linewidths, $^{17}\Gamma$, obtained from the high shift side of the spectra are plotted in Fig. 8 (open circles) where it can be seen that $^{17}\Gamma$ displays a Curie-like temperature dependence similar to that observed in underdoped $\text{YBa}_2(\text{Cu}_{1-z}\text{Ni}_z)_3\text{O}_{7-\delta}$. Also shown in Fig. 8 is the $\text{YBa}_2(\text{Cu}_{0.9825}\text{Zn}_{0.0175})_4\text{O}_8$ ^{89}Y NMR linewidth from the main peak, attributed to ^{89}Y remote from the Zn impurity (open triangles), where it can be seen that linewidths from both the Zn and Ni substituted samples have a similar temperature dependence. This would seem to indicate that the origin of the temperature-dependent NMR linewidths is not related to a commensurate spin density oscillation induced by a local moment because the sizes of the Ni moment ($1.5\mu_B/\text{Ni}$ to $3.4\mu_B/\text{Ni}$) and the assumed Zn induced moment ($1.04\mu_B/\text{Zn}$) are so different and, in the case of Zn, the moment is assumed to be distributed on the four Cu sites nearest neighbor to the Zn impurity.

The effect of combined Ni and Zn cosubstitution can be seen in Fig. 9 where we plot the ^{89}Y NMR spectra from $\text{YBa}_2(\text{Cu}_{1-z}\text{Zn}_{0.00875}\text{Ni}_{0.00875})_4\text{O}_8$ with the same total impurity concentration as $\text{YBa}_2(\text{Cu}_{0.9825}\text{Zn}_{0.0175})_4\text{O}_8$ and $\text{YBa}_2(\text{Cu}_{0.9825}\text{Ni}_{0.0175})_4\text{O}_8$ at (a) 133 K and (b) 293 K. The spectra clearly display intensity in the region of the $\text{YBa}_2(\text{Cu}_{0.9825}\text{Zn}_{0.0175})_4\text{O}_8$ satellite peaks. This is apparent

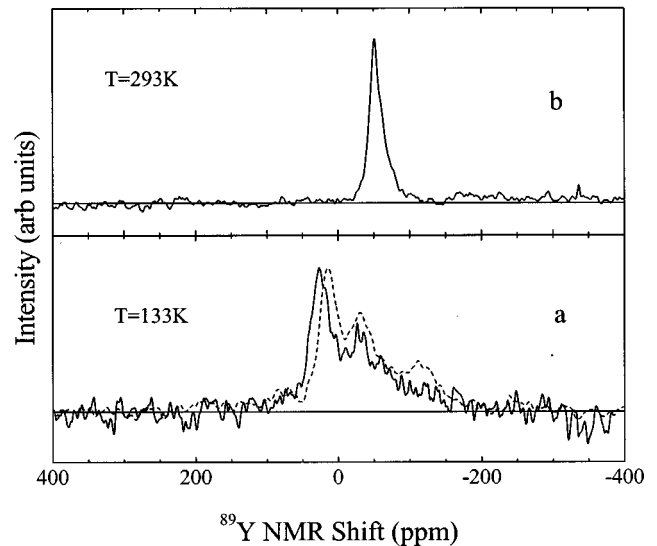


FIG. 9. Plot of the ^{89}Y NMR MAS spectra from $\text{YBa}_2(\text{Cu}_{0.9825}\text{Zn}_{0.00875}\text{Ni}_{0.00875})_4\text{O}_8$ at (a) 133 K and $D_0=60$ s and (b) at 293 K. Also included in (a) is the $\text{YBa}_2(\text{Cu}_{0.9825}\text{Zn}_{0.0175})_4\text{O}_8$ ^{89}Y NMR spectra at 132 K (dashed curve).

in Fig. 9(a) where we also plot the ^{89}Y NMR spectra from $\text{YBa}_2(\text{Cu}_{0.9825}\text{Zn}_{0.0175})_4\text{O}_8$ (dashed curve). Furthermore, it is apparent in Fig. 4 that the resultant NMR shifts of the main peak and the first satellite peak are also close to those observed in $\text{YBa}_2(\text{Cu}_{0.9825}\text{Zn}_{0.0175})_4\text{O}_8$ and $\text{YBa}_2(\text{Cu}_{0.9825}\text{Ni}_{0.0175})_4\text{O}_8$. This would seem to imply that the main peak and the first satellite peak originate from ^{89}Y away from the Zn impurity and Zn that is next-nearest neighbor to the Zn impurity respectively. The appearance of a Zn related satellite peak at the position found in $\text{YBa}_2(\text{Cu}_{0.9825}\text{Zn}_{0.0175})_4\text{O}_8$ establishes an upper limit for the extent of any commensurate spin density oscillation induced by the Ni moment. The average Zn-Ni separation of $\sim 5a$ per CuO_2 plane implies an ξ of $\xi < 1$ otherwise the Zn satellite peak would be shifted and broadened by the commensurate spin density oscillation.

CONCLUSION

In conclusion, we find three peaks in the $\text{YBa}_2(\text{Cu}_{1-z}\text{Zn}_z)_4\text{O}_8$ ^{89}Y NMR spectra that can be analyzed in terms of a Curie-like shift from Cu sites that are adjacent to the Zn impurity. This analysis is consistent with the ^{17}O NMR spectra from $\text{YBa}_2(\text{Cu}_{1-z}\text{Zn}_z)_4\text{O}_8$. We find that the Curie-like NMR shift is washed out in the ^{89}Y and ^{17}O NMR spectra from $\text{YBa}_2(\text{Cu}_{1-z}\text{Ni}_z)_4\text{O}_8$ due to the Ni moment. We find problems in attributing the Curie-like shift to an induced local moment. In particular, the NMR data from Zn, Ni, and Zn:Ni substituted into $\text{YBa}_2\text{Cu}_4\text{O}_8$ are inconsistent with a spin-density oscillation about an induced local moment, or even about the Ni moment, of the radius assumed.

ACKNOWLEDGMENTS

We acknowledge funding support from the New Zealand FRST (G.V.M.W.), The Royal Society of New Zealand (J.L.T.), and the United Kingdom EPSRC (R.D.).

- ¹D. Pines, *Physica C* **282-287**, 273 (1997).
- ²A. V. Mahajan, H. Alloul, G. Collin, and J. F. Marucco, *Phys. Rev. Lett.* **72**, 3100 (1994).
- ³B. Nachurni, A. Keten, K. Kojima, M. Larkin, G. M. Luke, J. Merrin, O. Tchernysköv, Y. J. Uemura, N. Ichikawa, M. Goto, and S. Uchida, *Phys. Rev. Lett.* **77**, 5421 (1996).
- ⁴C. Bernhard, J. L. Tallon, C. Bucci, R. De Renzi, G. Guidi, G. V. M. Williams, and Ch. Niedermayer, *Phys. Rev. Lett.* **77**, 2304 (1996).
- ⁵J.-S. Zhou, J. B. Goodenough, and B. Dabrowski, *Phys. Rev. B* **58**, 2956 (1998).
- ⁶P. Mendels, H. Alloul, J. H. Brewer, G. D. Morris, T. L. Dutty, S. Johnston, E. J. Ansaldo, G. Collin, J. F. Marucco, Ch. Niedermayer, D. R. Noakes, and C. E. Stonach, *Phys. Rev. B* **49**, 10 035 (1994).
- ⁷C. Bernhard, Ch. Niedermayer, T. Blasius, G. V. M. Williams, R. De Renzi, C. Bucci, and J. L. Tallon, *Phys. Rev. B* **58**, 8937 (1998).
- ⁸G. V. M. Williams, J. L. Tallon, R. Dupree, and R. Michalak (unpublished).
- ⁹G. V. M. Williams and J. L. Tallon, *Phys. Rev. B* **57**, 10 984 (1998).
- ¹⁰F. Bridges, J. B. Boyce, T. Claeson, T. H. Geballe, and J. M. Tarascon, *Phys. Rev. B* **42**, 2137 (1990).
- ¹¹C. Y. Yang, A. R. Moodenbaugh, Y. L. Wang, Youwen Xu, S. M. Heald, D. O. Welch, M. Sueaga, D. A. Fischer, and J. E. Penner-Hann, *Phys. Rev. B* **42**, 2231 (1990).
- ¹²J. W. Loram (unpublished); see also, J. R. Cooper, in *IRC Superconductivity Research Review*, edited by W. Y. Liang (Cambridge University Press, Cambridge, England, 1994).
- ¹³K. Ishida, Y. Kitaoka, N. O. Gata, T. Kamino, K. Asayama, J. R. Cooper, and N. Athanassopoulou, *J. Phys. Soc. Jpn.* **62**, 2803 (1993).
- ¹⁴J. Bobroff, H. Alloul, Y. Yoshinari, A. Keren, P. Mendels, N. Blanchard, G. Collin, and J. F. Marucco, *Phys. Rev. Lett.* **79**, 2117 (1997).
- ¹⁵R. E. Walstedt, R. F. Bell, L. F. Schneemeyer, J. V. Waszczak, W. W. Warren, R. Dupree, and A. Gencten, *Phys. Rev. B* **48**, 10 646 (1993).
- ¹⁶J. L. Tallon, C. Bernhard, G. V. M. Williams, and J. W. Loram, *Phys. Rev. Lett.* **79**, 5294 (1997).
- ¹⁷G. V. M. Williams, E. M. Haines, and J. L. Tallon, *Phys. Rev. B* **57**, 146 (1998).
- ¹⁸F. Mila and T. M. Rice, *Physica C* **157**, 561 (1998).
- ¹⁹M. Mehring, *Appl. Magn. Reson.* **3**, 383 (1992).
- ²⁰M. Takigawa, W. L. Hults, and J. L. Smith, *Phys. Rev. Lett.* **71**, 2650 (1993).
- ²¹R. Dupree, Z. P. Han, D. McK. Paul, T. G. N. Babu, and C. Greaves, *Physica C* **179**, 355 (1991).
- ²²G. V. M. Williams, D. J. Pringle, and J. L. Tallon (unpublished).
- ²³S. Zagoulaev, P. Monod, and J. Jégoudez, *Phys. Rev. B* **52**, 10 474 (1995).
- ²⁴N. J. Curro, T. Imai, C. P. Scichter, and B. Dabrowski, *Phys. Rev. B* **56**, 877 (1997).
- ²⁵C. Coretsopoulos, H. C. Lee, E. Ramli, L. Reven, T. B. Rauchfuss, and E. Oldfield, *Phys. Rev. B* **39**, 781 (1989).
- ²⁶M. Takigawa, C. Hammel, R. H. Heffner, Z. Fisk, K. C. Ott, and J. D. Thompson, *Phys. Rev. Lett.* **63**, 1865 (1989).
- ²⁷G. V. M. Williams, J. L. Tallon, R. Michalak, and R. Dupree, *Phys. Rev. B* **57**, 8696 (1998).
- ²⁸R. Liang, T. Nakamuar, H. Kawaji, M. Itoh, and T. Nakamura, *Physica C* **170**, 307 (1990).
- ²⁹P. Mendels, H. Alloul, G. Collin, N. Blanchard, J. F. Marucco, and J. Bobroff, *Physica C* **235-240**, 1595 (1994).
- ³⁰T. H. Meen, F. L. Juang, W. J. Huan, Y. C. Chen, K. C. Huang, and H. D. Yang, *Physica C* **242**, 373 (1995).